The response surface methodology approach successfully optimizes a dry milling process of porang (*Amorphophallus muelleri* Blume) flour production that uses micro mill- assisted by cyclone separator

J. E. Witoyo[1,4], B. D. Argo[2], S. S. Yuwono[3], S. B. Widjanarko[3,4]*

(1. Alumni Master Student of Department of Food Science and Biotechnology, Faculty of Agricultural Technology, University of Brawijaya. Malang 65145, Indonesia;

2. Bioprocess Engineering, Department of Biosystem Engineering, Faculty of Agricultural Technology, University of Brawijaya, Malang 65145, Indonesia;

3. Department of Food Science and Biotechnology, Faculty of Agricultural Technology, University of Brawijaya. Malang 65145, Indonesia ;

4. Porang Research Center, Universitas Brawijaya, Malang 65145, Indonesia)

Abstract: The purpose of this study was to determine the effects of feed rate and inlet air velocity on the physicochemical properties of porang flour by using Central Composite Design Method of Response Surface Methodology (CCD –RSM), in order to ascertain whether the CCD-RSM as a predictive approach is accurate in optimizing porang flour production. Advanced instruments, including FTIR (Fourier-transform Infrared Spectroscopy), SEM (Scanning Electron Microscopy), DSC (Differential Scanning Calorimetry), XRD (X-Ray Diffraction), and PSA (Particle Size Analyzer) were used to characterize an optimum micro-mill milled porang flour (OMMPF). The optimum conditions for producing porang flour were feed rate of 48.86 kg h^{-1}, and an inlet air velocity of 9.00 m s^{-1}, which produced a calcium oxalate content of 2.45%±0.03%, a degree of whiteness (DoW) of 56.90±0.17, a viscosity of 4031.30±54.10 cPs, and a glucomannan content of 53.29% ±0.22% dry bases (d.b). OMMPF had an amorphous form based on the XRD-Diffraction analysis. DSC analysis revealed that first and second peaks were at 99.50℃ - 101.90℃ and 310.20℃ - 316.80℃, respectively. Particle size analysis of OMMPF was in the range 238.63 - 467.48 μm. We conclude that the Response Surface Methodology is an accurate approach for optimizing porang flour production.

Keywords: Micro-mill, *Amorphophallus muelleri* Blume, response surface methodology, dry milling, DSC, SEM

Citation: Witoyo, J. E.,Argo, B.D., Yuwono, S.S., and Widjanarko, S.B. 2023. The response surface methodology approach successfully optimizes a dry milling process of porang (*Amorphophallus muelleri* Blume) flour production that uses micro mill-assisted by cyclone separator. Agricultural Engineering International: CIGR Journal, 25(1): 176-190.

1 Introduction

Porang (*Amorphophallus muelleri* Blume) is one of the native plants of the tropical plains of East and Southeast Asia, including Japan, China, Thailand, Myanmar, and Indonesia (Impaprasert et al., 2014). In Indonesia, Porang production reaches 8704.95 tons per year (Central Bureau of Statistics of Madiun Regency, 2018), and the plant is known to have a high glucomannan content. Glucomannan is the most abundant heteropolysaccharide in nature and can be found in

Received date: 2020-08-17 **Accepted date:** 2022-08-12

***Corresponding author: S. B. Widjanarko,** Professor of Food Science and Technology, Department of Food Science and Biotechnology, Universitas Brawijaya, Malang, Indonesia. Tel: +62-341-569214, Fax: +62-341-569214. E-mail: simonbw@ub.ac.id.

hemicellulose, bulbil, roots, and tubers, which are water soluble, have high viscosity and are easily fermented (Alonso-Sande et al., 2009). Structurally, konjac glucomannan is composed of units of D-glucose and D-mannose, which are linked by the β-1,4 glycosidic bond with a small number of acetyl groups (Wang et al., 2012). Generally, the glucose and mannose molar ratios are 1:1.6 or 2:3 (Alonso-Sande et al., 2009) with a degree of polymerization of 6000 (Behera and Ray, 2017). However, utilization of porang is limited due to the presence of toxic compounds known as calcium oxalate (Widjanarko et al., 2014), so that the process of separating glucomannan and calcium oxalate needs to be done to obtain pure porang flour and expand its application in both the food and non-food fields (Zhang et al., 2014).

Micro-mill is basically a hammer mill that has a double jacket wall. The double jacket wall contains tap water that flows in and out of the wall of a micro-mill because of the works of a water pump. The purpose of making the double jacket wall to surround the milling chamber is to reduce the heat build-up during the milling process of porang chips. A micro-mill grinder equipped with the double jacket wall has the advantage of being able to grind fibrous or brittle materials, producing diverse particle sizes (Basiouny and El-Yamani, 2016), and requires little energy during the process (Chițoiu et al., 2016). Some researchers have applied the hammer mill for milling of food and non-food products with different factors (Tumuluru et al., 2014; Basiouny and El-Yamani, 2016; Chițoiu et al., 2016). On the other hand, the fractionation of materials based on size or density, especially for flour products, generally uses cyclone separators (Surjosatyo et al., 2017). Marinuc and Rus (2011) noted that theoretically the efficiency of the separation was more effective at the high input velocity in a cyclone separator with a small cyclone inlet section.

Applications of cyclone separators can be found in the chemical, mining, and burning industries (Avci et al., 2013), but it is still rarely applied to the food industry. The first information about the effect of feed rate and inlet air velocity on porang flour characteristics was provided by (Witoyo et al., 2019), who claimed that the feed rate and inlet air velocity were effective in reducing calcium oxalate on the porang chips to produce porang flour, but no further information was provided on their effect on the other responses such as glucomannan content and viscosity. Previous studies reported that the feed rate affects the separation process of impurities in other agricultural products (Simonyan et al., 2006; Sugiono et al., 2019). In other factors, inlet air velocity also significantly affects the process of separating glucomannan and non-glucomannan during the porang chips milling process accompanied by air fractionation. The recommended inlet air velocity in cyclone separator for processing porang flour is 5 to 9 m s^{-1} to obtain low calcium oxalate and high glucomannan content (Hermanto et al., 2019).

Response surface methodology (RSM) is a collection of statistical and mathematical techniques used for the development, modeling and optimization of chemical and biochemical processes (Baş and Boyacı, 2007). Conceptually, this method is used to obtain the optimal point of a process without requiring too much data (Widyaningsih et al., 2018). This paper reports the effect of the feed rate and inlet air velocity on the physicochemical properties of porang flour by using central composite design method of response surface methodology (CCD –RSM), in order to ascertain whether the CCD-RSM as a predictive approach is accurate in optimizing porang flour production and on its other structural properties.

2 Materials and methods

2.1 Materials

Porang chips (Figure 1a), which were free from dirts and had 12% moisture content, were obtained from Kepel Village, Kare District, Madiun Regency, East Java, Indonesia. The research location was conducted in the Pilot Plant Laboratory, Faculty of Agricultural

Technology, Universitas Brawijaya, and the porang flour were analyzed in the Food Chemical and Biochemical Laboratory, Faculty of Agricultural Technology, Universitas Brawijaya, Malang. All chemical reagents of analytical grade were purchased from Merck KgaA (Darmstadt, Germany). The schematic drawing of the micro mill assisted cyclone separator is shown in Figure 2. The feed rate was controlled with the manipulation of the speed of the feeder screw connected to a 3-phase motor by an inverter (Danfoss VLT 500 C/M Ersa CD-2-2). The frequency ranged from 10.5 Hz – 14.2 Hz and was controlled manually to obtain the optimum feed rate condition of the micro-mill during the milling processes of crude konjac flour. The optimum feed rate condition was determined by a mass of crude porang flour (CPF) that came out from the feeder screw for every 5 minutes at each frequency. The output product was collected and weighed, to get the feed rate in units of kg h^{-1}. The preliminary trials at the frequencies of 10.7 Hz, 11.3 Hz, 12.5 Hz, 13.7 Hz, and 14.2 Hz resulted in feed rate conditions of 42.93 kg h^{-1}, 45 kg h^{-1}, 50 kg h^{-1}, 55 kg h^{-1}, and 57.07 kg h^{-1}, respectively. The inlet air velocity was controlled using a manual valve, namely the Inlet exhausted blower (Figure 2, No. 2), and measured using a hand anemometer (Genetech GM 816) (Witoyo et al., 2019).

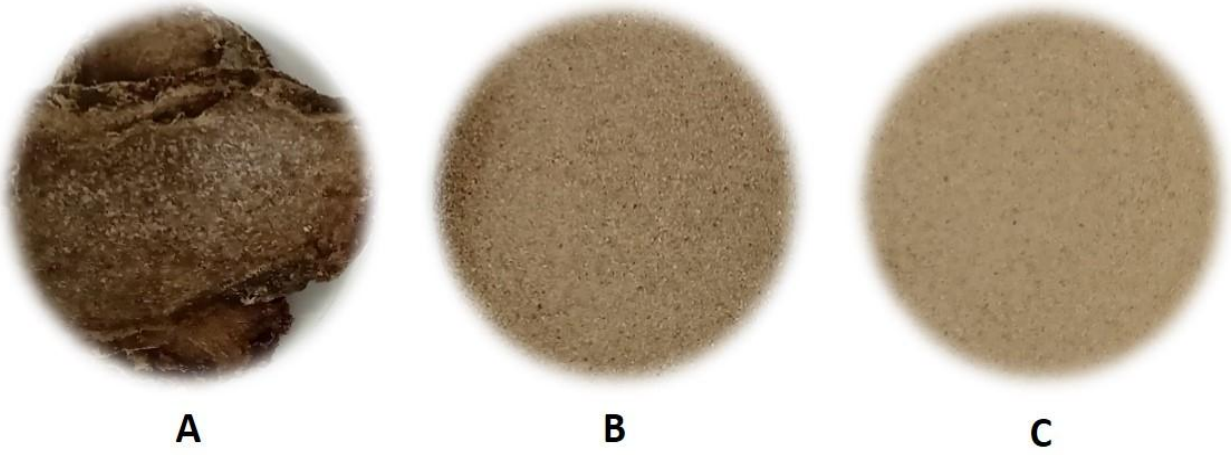

Figure 1 The porang chips (a), the crude porang flour (CPF) (b) and the optimum micro-mill milled porang flour (OMMPF) (c)

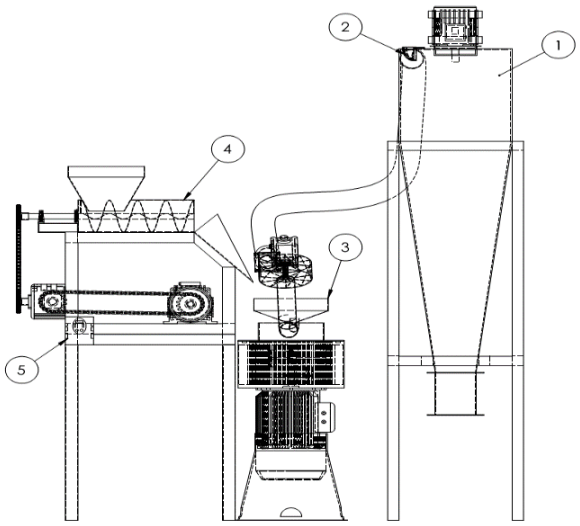

Cyclone Separator, (2) Manual Valve, (3) micro mill, (4) feeder screw, (5) Inverter

Figure 2 The schematic drawing of micro mill assisted by cyclone separator

2.2 Dry milling process

The dry milling process of porang chips was described by (Witoyo et al., 2019). The milling process procedure is as follows: porang chips at 12% ±0.01% moisture content w.b. were ground using a disk mill (FFC 45 Model) with a 20 mesh sieve as first grinding treatment and the output was named a CPF. CPF was used as an input for the second dry milling process. About 2 kg of CPF was milled with a micro-mill grinder (locally made, the diameter: 25 cm, height: 15 cm, number of hammer: 6 (the cross section of each hammer: 5 cm of length and 2 cm of height), 2850 rpm of motor rotational speed, and the millig capacity of 60 kg h^{-1}) connected to a cyclone separator (model 1D3D, based on Wang et al.'s study (Wang, 2004)) (Figure 2). The micro-mill grinder had a 40 mesh steel screen. The milling process conditions of the micro-mill grinder with regard to the feed rate and inlet air velocity were used as stated in the "Design of Experiment (DoE)" in Table 1. Each milling process produced 2 fractions of porang flour, namely heavy fraction (passed through 40 mesh sieve) and light fraction. The heavy fraction containing glucomannan was stored and analyzed further.

2.3 Experimental design and statistical analysis

The milling of porang chips experiment was designed based on CCD-RSM with 2 independent variables, namely, feed rate (X_1) and inlet air velocity of cyclone separator (X_2). A Factorial, an axial and central point of independent variable were as presented in Table 1. The 13 runs of milling were conducted in a randomized order and the data were analyzed by multivariate analysis using Design Expert 10 trial version (State Ease Inc., Minneapolis, USA). The non-linear model of the system was calculated by the quadratic equation as followed by Equation 1 (Widjanarko et al., 2014).

$$Y = \beta_0 + \sum_{i=1}^{k} \beta_i X_i + \sum_{i=1}^{k} \beta_{ii} X_i^2 + \sum_{i=1,j=2}^{k-1,k} \beta_{i,j} X_i X_j + \varepsilon \quad (1)$$

where, Y is the observed response, β_0, β_i, β_{ii}, and β_{ij} are the regression coefficients of the intercept, linearity, quadratic, and interaction of the treatment, respectively. X_i and X_j are the coded independent variables, and k is the number of independent parameters, and ε is a random error. The polynomial coefficient of the quadratic model was obtained from the Design Expert 10 trial version program (State Ease Inc, Minneapolis, USA). The lack of fit, R^2 value, adjusted R^2 value and coefficient of variation (CV) value were used to find the appropriate model for a response. Data verification was compared between software prediction and laboratory experimental values using the paired T-test by Minitab 17.0 trial version.

Table 1 Range of dry milling process of porang chips

Independent Variable	Unit	-α	-1	0	+1	+ α
X_1: feed rate	kg h^{-1}	42.93	45	50	55	57.07
X_2:inlet air velocity	m s^{-1}	4.17	5	7	9	9.83

2.4 Determination of physicochemical properties of porang flour

2.4.1 Calcium oxalate content determination

Calcium oxalate in the porang flour was determined based on the methods of Ukpabi and Ejidoh (1989) as reported in Iwuoha and Kalu (1995) with minor modification. Briefly, 2 g of porang flour was added to 190 mL of distilled water and 10 mL of 6M HCl in a volumetric flask. The mixed solution was heated at 100°C for 1 hour and then cooled. The mixed solution was diluted with distilled water to a volume of 250 mL, then filtered to obtain the filtrate. The resulting filtrate was divided into 2 parts (125 mL each). Then, to each filtrate was added 4 drops of methyl red and ammonium hydroxide (NH_4OH) indicators until the color changed from pink to yellow, followed by heating until the temperature reached 90°C, after which it was then cooled

and filtered. The filtrate was reheated until the temperature reached 90°C, then 10 mL of 5% $CaCl_2$ was added and stirring was done with a magnetic stirrer for 3 minutes, followed by overnight storage at 5°C. Then, each filtrate was centrifuged at 8000 rpm for 15 minutes until the supernatant and pellet were separated. The pellet was dissolved with 10 mL of 20% H_2SO_4 so that 10 mL of the filtrate was obtained. Both parts of the filtrate (each 10 mL) were mixed and diluted with distilled water to 250 mL. 125 mL of the resulting filtrate was then heated to almost boiling. Furthermore, it was immediately titrated in hot conditions with a standardized 0.05 M $KMnO_4$ until a pink color was formed and persisted for 30 seconds. Calcium oxalate content (%) in the porang flour was calculated by Equation 2.

$$Calcium\ Oxalate\ Content\ (\%) = \frac{T \times V_{me} \times D_f \times 10^5}{ME \times M_f \times 1000} \quad (2)$$

where, T is the volume of $KMnO_4$ used for titration (mL), V_{me} is the equivalent mass volume (1 cm^3 0.05 M $KMnO_4$, equivalent to 0.00225 g anhydrous oxalic acid), D_f is the dilution factor, ME is the molar equivalent of $KMnO_4$ solution (0.05), and M_f is the mass of the porang flour (g).

2.4.2 Glucomannan content determination

The glucomannan content of porang flour was determined using the method described by Chua et al. (2012) with modifications. The glucomannan content was calculated by Equation 3.

$$\text{GM content (\% d.b)} = \frac{0.9 \times (5T - T_0) \times fp}{m \times (100 - w)} \quad (3)$$

where, m is the mass of porang flour (200 mg), w is water content of porang flour, T_o is glucose content of porang flour extract (mg), T is glucose content of porang flour hydrolysate (mg), and f_p is dilution factor.

2.4.3 Degree of whiteness determination

The values of L, a^* and b^* of porang flour were evaluated by color reader CR-10 (Minolta, Japan). Porang flour was inserted into the acrylic cylinder and its value was measured. The degree of whiteness of porang flour was calculated using Equation 4 (Impaprasert et al., 2014).

$$W = 100 - ((100 - L) \times 2 + (a^2 + b^2))^{0.5} \quad (4)$$

where, W is degree of whiteness, assuming the value 100 is the most whiteness), L is lightness, a^* is redness (+)/greeness (-), b^* is yellowness (+)/blueness(-).

2.4.4 Viscosity determination

The method reported in Yanuriati et al. (2017) with modifications for determining the viscosity of porang flour was used. Briefly, 1% of a porang flour solution was dissolved using a magnetic stirrer with an agitation speed of 150 rpm at a constant temperature (75 ℃) until perfectly hydrated. The measurements of viscosity were performed at room temperature (25 ℃-30 ℃) using Manual Rotational Viscometer NDJ-1 on spindle 4 and agitation speed 12 rpm.

2.5 Structural characteristics

2.5.1 Microstructure

Microstructural analysis of CPF and OMMPF was done according to the method of (Xu et al., 2014). CPF and OMMPF samples were placed on top of a stub, and coated with gold-palladium before observation. The coated samples were determined using SEM-EDX Merk FEI type Inspect S50 (Japan) in accelerating voltage of 20 kV. The magnification was displayed on the micrograph.

2.5.2 X-ray diffraction (XRD)

The XRD patterns of CPF and OMMPF were determined using a PANalytical X'Pert Pro (40 kV and 35 mA) with a scan rate of 4 ℃ min^{-1}. The diffraction angles used ranged from 10 °to 50 °.

2.5.3 Functional group determination

Measurements of functional groups from CPF and OMMPF were done as reported by (Widjanarko et al., 2011). The FTIR spectrum of flour porang was recorded by Shimadzu FTIR Fourier Transform Infrared Spectrophotometer- 8400 S. Briefly, 0.01 g of porang flour sample was homogenized with 0.01 g KBr

anhydrous and pressed using a hydraulic vacuum (Graseby Specac) on 1.2 psi to obtain a pellet. Furthermore, pellets of CPF and OMMPF were scanned using a frequency range of 400 to 4000 cm^{-1}.

2.5.4 Thermal properties

Thermal properties of CPF and OMMPF were observed using the method described by (Li et al., 2005). DSC analysis was carried out using an Exstar 7000 DSc Series instrument (SciMed Ltd., UK). 1 gram of porang flour was placed on the crucible with a reference sample of aluminum in another crucible to be heated at a constant rate of 10 ℃ min^{-1} in the temperature range of 30 ℃ - 400 ℃ under the conditions of the nitrogen atmosphere with a flow rate of 25 mL min^{-1}.

2.5.5 Particle size analysis

Particle size of OMMPF sample was evaluated using a particle size analyzer (CILAS 1090D) (Manab et al., 2017).

Table 2 Physicochemical properties of porang flour for each experimental run using CCD- RSM

Std	Run	Actual Variable		Coded Variable		Responses			
		Feed Rate (Kg h^{-1})	Inlet Air Velocity (m s^{-1})	X_1	X_2	Calcium Oxalate (%)	Degree of Whiteness	Viscosity (cPs)	Glucomannan Content (% d.b)
13	1.	50.00	7.00	0.00	0.00	2.51	56.57	4250.00	52.96
7	2.	50.00	4.17	0.00	-1.41	3.17	55.98	3093.75	42.38
11	3.	50.00	7.00	0.00	0.00	2.62	56.56	4187.50	53.34
2	4.	55.00	5.00	1.00	-1.00	3.06	55.74	2781.25	40.99
6	5.	57.07	7.00	1.41	0.00	2.95	55.97	2812.50	40.50
12	6.	50.00	7.00	0.00	0.00	2.62	56.53	3937.50	52.22
8	7.	50.00	9.83	0.00	1.41	2.40	57.09	4218.75	53.55
1	8.	45.00	5.00	-1.00	-1.00	2.95	56.41	3343.75	44.81
3	9.	45.00	9.00	-1.00	1.00	2.59	57.23	3531.25	49.59
10	10.	50.00	7.00	0.00	0.00	2.51	56.61	4187.50	53.97
5	11.	42.93	7.00	-1.41	0.00	2.95	57.05	2812.50	42.30
4	12.	55.00	9.00	1.00	1.00	2.62	56.74	2968.75	42.96
9	13.	50.00	7.00	0.00	0.00	2.51	56.44	3968.75	51.28

Note: * no unit (100 corresponds to 'pure white')

Table 3 Analysis of variance of the second polynomial order for calcium oxalate, degree of whiteness, viscosity, and glucomannan content of porang flour

Source of Variation	p-value >F			
	Calcium Oxalate	Degree of Whiteness	Viscosity	Glucomannan Content
Model-Quadratic	0.0002***	< 0.0001***	0.0022**	0.0005***
X_1	0.4885^{ns}	< 0.0001***	0.1522^{ns}	0.0370*
X_2	< 0.0001***	< 0.0001***	0.0272*	0.0029**
X_1X_2	0.5940^{ns}		1.0000^{ns}	0.4563^{ns}
X_1^2	0.0003***		0.0002***	<0.0001***
X_2^2	0.0078**		0.0363*	0.0091**
Lack of Fit	0.2725^{ns}	0.3669^{ns}	0.0608^{ns}	0.0658^{ns}
R^2	0.9530	0.9793	0.8995	0.9369
Adj R^2	0.9194	0.9751	0.8277	0.8919
CV (%)	2.60	0.12	7.04	3.74

Note : *p<0.05, **p<0.01 ***p<0.001, ^{ns} not significant, X_1 : Feed rate of milling (kg h^{-1}), X_2 : Inlet air velocity (m s^{-1}), CV : coefficient of variation

3 Results and discussion

Response data of calcium oxalate (Y_1), degree of whiteness (Y_2), viscosity (Y_3), and glucomannan (Y_4) content obtained from this study are shown in Table 2. Furthermore, the results of the analysis of variance (ANOVA) are listed in Table 3. The analysis of variance (ANOVA) as listed in Table 3 showed that quadratic models represented responses of the calcium oxalate, viscosity, and glucomannan content. However, the degree of whiteness was followed by the linear model. The coefficients of determination (R^2) for the calcium oxalate, degree of whiteness, viscosity, and glucomannan responses were 0.9530, 0.9793, 0.8995, and 0.9369, respectively. Furthermore, the adjusted R^2 of 0.9194 for

calcium oxalate, 0.9751 for the degree of whiteness, 0.8277 for viscosity, and 0.8919 for glucomannan were obtained. The high value of the coefficient of determination (R^2) and Adjusted R^2 indicated that many variations of the observed responses could be predicted and explained by the obtained model (Pasandide et al., 2017). In addition, all the responses had a low CV, which was less than 5%, except for the viscosity response (Table 3). The low CV values indicated the level of reliability, and the precision of experimental data was very good (Zhu and Liu, 2013). The lack of fit value was non-significant ($p > 0.05$) for all responses. The lack of fit values of the responses were 0.2725, 0.3669, 0.0928, and 0.0658 for calcium oxalate, the degree of whiteness, viscosity, and glucomannan content, respectively. The statistical non-significance of the lack of fit indicated the appropriate model for predicting the extraction process (Chen and Xue, 2019). The quadratic mathematical models for representing the correlation between the independent variables and the response of calcium oxalate (Y_1), degree of whiteness (Y_2), viscosity (Y_3), and glucomannan (Y_4) of porang flour are shown in Equations 5-8, respectively. The 3D-surface response graphs for all porang flour responses are shown in Figure 3.

$$Y1 = 2.56 + 0.018X1 – 0.24X2 -0.020X1X2 + 0.18X12 + 0.099 X22 \quad (5)$$

$$Y2 = 56.53- 0.34X1+ 0.42 X2 \quad (6)$$

$$Y3 = 4106.25 – 140.62X1 + 245.75 X2 +0.00 X1X2- 666.41 X12- 244.53X22 \quad (7)$$

$$Y4 = 52.75- 1.62X1+ 2.82X2- 0.70 X1X2 -0.570X12- 2.42X22 \quad (8)$$

3.1 Effects of feed rate and inlet air velocity on the responses

3.1.1 Calcium oxalate and glucomannan content

Calcium oxalate is one of the impurities that must be removed from porang flour to get pure porang flour with high glucomannan content. Figure 3 (A and D) and Table 3 explain calcium oxalate and glucomannan content of porang flour were significantly affected by feed rate and inlet air velocity. In this present study, the feed rate had a quadratic effect, whereas the inlet air velocity had a linear and quadratic effects on the calcium oxalate and glucomannan content of porang flour. The minimum calcium oxalate obtained through 50 kg h^{-1} of feed rate, and increased dramatically afterwards (Figure 3A). In contrast, the reverse phenomenon was found with the glucomannan response (Figure 3D). The glucomannan content increases as the feed rate increases until 50 kg h^{-1} but decreases afterward. Increasing feed rate of food materials into a barrel of an extruder to a certain point can increase the contact of food materials with the screw (Sugiono et al., 2019). Ultimatetly, this process can remove impurities (i.e. calcium oxalate) which adhere to the surface of glucomannan granules. However, an increase in the excessive optimal feed rate is thought to be able to reduce contact and result in a less optimum separation process (Simonyan et al., 2006). Moreover, the observed patterns of the effects of feed rate on calcium oxalate are consistent with the earlier research conducted by (Witoyo et al., 2019). Equation 5 and Equation 8 show that the inlet air velocity had a negative linear correlation with the calcium oxalate and a positive linear correlation with the glucomannan content of porang flour. This model means that increasing inlet air velocity will increase glucomannan content but decrease calcium oxalate content. Moreover, the inlet air velocity also had quadratic effect on the calcium oxalate, and glucomannan content of porang flour. These results are in agreement with Marinuc and Rus (2011) that reported the separation process was effective at high inlet air velocities. Gupta (2013) noted the efficiency of cleaning moong beans from impurities increases with an increase in air velocity and a decrease in feed rate. Aderinlewo et al. (2016) reported that the impurities from cowpea were reduced at high air velocity using rotary screen cleaner, with the efficiency of separation process being more than 80%.

3.1.2 Degree of whiteness

Figure 3 (B) and Table 3 explain that the feed rate and inlet air velocity had a significant effect

on the degree of whiteness (DoW) of porang flour. Equation 6 shows that the feed rate caused a negative linear trend to the DoW of porang flour. The linear trend is similar to previous results obtained (Wardhani et al., 2016). Lowering feed rate during the grinding process was able to reduce the grinding load in the milling zone. Scanlon and Dexter (1986) reported that the consequence of lowering grinding conditions by reducing a feed rate is an increase in the intensity of collisions between materials and smooth rolls of a grinder. Furthermore, high intensity will separate the bran from the material endosperm, and increase the color of the milled material. In addition, Al-sadi (2017) noted that color increases with a decrease in feed rate in the preparation process for making polycarbonate. Moreover, the inlet air velocity caused a positive linear trend to the DoW of porang flour (Equation 6). The DoW of porang flour was increased as a function of increased inlet air velocity. The porang flour showed more brightness with low feed rate and high inlet air velocity. Increasing inlet air velocity was able to enhance the degree of whiteness of porang flour. Mawarni and Widjanarko (2015) reported that increase in the porang flour brightness causes a decrease in the amount of impurities that adhere to porang flour granules. Moreover, the observed patterns of the effects of feed rate on DoW are consistent with the earlier research conducted by (Witoyo et al., 2019).

3.1.3 Viscosity

The independent variables used affected the viscosity of porang flour. The feed rate had a quadratic significant effect on the viscosity of porang flour, but the inlet air velocity had a linear and quadratic significant effects (Table 3). Figure 3C shows the viscosity of porang flour was increased until the feed rate reached 50 kg h^{-1}, after which the viscosity decreased. On the other hand, the inlet air velocity had a positive linear and quadratic correlation with the viscosity of porang flour (Equation 7). A similar quadratic model of the effect of feed rate on the viscosity was reported by Sugiono et al. (2019). The viscosity of porang flour was increased with increase in inlet air velocity (Figure 2C). This data shows that increasing the inlet air velocity was able to remove impurities. In this study, the viscosity of porang flour was lower than that reported by (Faridah and Widjanarko, 2013; Widjanarko et al., 2014) as well as for konjac flour standards (Liu et al., 2002). This phenomenon may be due to the particle size of porang flour, which was a 40 mesh sieve. Faridah and Widjanarko (2013), Widjanarko et al. (2014), and Faridah (2016) mentioned that the particle sizes of their porang were more than 80 mesh. It is known that the larger the particle size of porang flour, the lower is the viscosity of its solution at the same time of making a solution. Uzombah and Awonorin (2010) reported that viscosity has a negative correlation with particle size in the process of making the paste from reconstituted flour (corn, sorghum and cowpea seeds). As shown in Table 2, end products of porang flour still contained many impurities, such as calcium oxalate, protein, starch and ash. So, the glucomannan granules in porang flour are not able to dissolve entirely in the water. Yanuriati et al. (2017) noted that the impurity component surrounding the glucomannan cell had a lower viscosity than glucomannan, thus affecting the final viscosity of the porang flour. Kurt and Kahyaoglu (2017a) reported that impurities such as protein, ash, starch, and other materials might disturbe the interaction between glucomannan and water, which was why a mixed solution containing glucomannan and its impurities showed low viscosity.

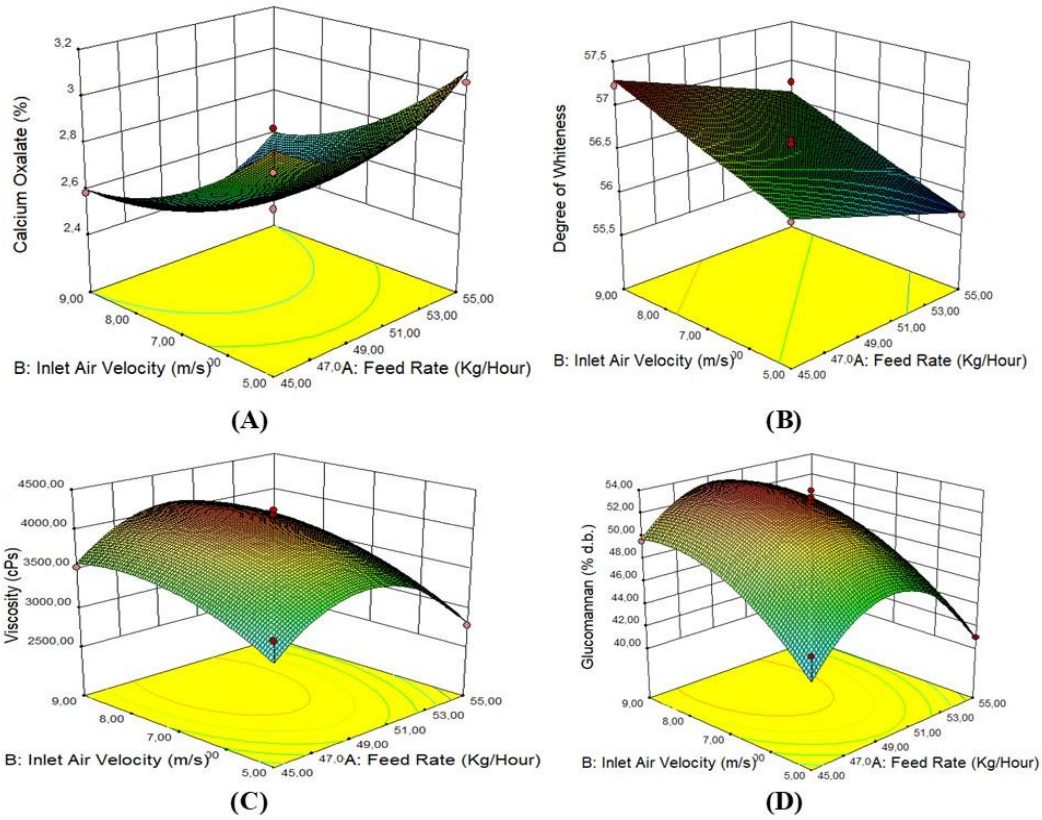

Figure 3 The effect of independent variables (feed rate and inlet air velocity) on calcium oxalate (A), degree of whiteness (B), viscosity (C), and glucomannan (D)

Table 4 The comparison between the prediction of DX software and laboratory experimental verification

	Feed Rate (kg h^{-1})	Inlet Air Velocity (m s^{-1})	Calcium Oxalate (%)	Degree of Whiteness	Viscosity (CPs)	Glucomannan (% d.b)	Desirability
Prediction	48.86	9.00	2.43±0.00	57.03±0.00	4104.80±1.50	53.39±0.00	0.922
Verification*	48.86	9.00	2.45±0.03	56.90±0.17	4031.30±54.10	53.29±0.22	-
	P-Value		0.468	0.291	0.143	0.522	-

Note: *Mean ± standard deviation (n=3)

3.1.4 Optimization and verification of prediction

In this research, we expected to produce porang flour with high glucomannan, high degree of whiteness, high viscosity, and low calcium oxalate. The criteria used for optimization in this study were ranges in the feed rate and the inlet air velocity, with each of the degree of whiteness, viscosity, and glucomannan set to a maximum. Calcium oxalate content was set to a minimum. Data from the prediction optimum analysis calculated by a DX software and verification data shown in Table 4 were compared. Based on Table 4, with regard to the four responses, there was no statistically significant difference (p >0.05) between the prediction and verification data. The optimum solution values as predicted by the software with respect to calcium oxalate, degree of whiteness, viscosity, and glucomannan content were 2.43%±0.00%, 57.03±0.00, 4104.80±1.50 cPs, and 53.39%±0.00% d.b., respectively, with desirability level of 0.922. These data are similar to the verification data from laboratory experiments, which were 2.45%±0.03% of calcium oxalate, 56.90±0.17 of degree of whiteness, 4031.10±54.10 cPs of viscosity, and 53.29%±0.22% d.b. of glucomannan. This provides evidence that the verification experiment supports the optimum point prediction and its validity. Similar results were reported by Sugiono et al. (2019).

3.2 Structural analyses

3.2.1 Microstructural analyses

Microstructural analyses of the KGM granules surface (CPF and OMMPF) were carried out using SEM. Figure 4 (A) shows that CPF had rough oval shape and was covered by a lot of clustering particles in the form of crumbs. Clustering particles on the surface of KGM were thought to be non-glucomannan compounds such as starch, protein, fat, ash and other impurities (Tatirat and Charoenrein, 2011; Xu et al., 2014; Wardhani et al., 2016). It is noted that Figure 4 (A3) shows needles of calcium oxalate and more impurities, while OMMPF granules at Figure 4 (B3) look clean, with smooth oval shape and less calcium oxalate needles. This data is in agreement with data reported by Faridah and Widjanarko (2013). Therefore, the micro-mill milling process for CPF to produce OMMPF indicates that dry milling process can reduce impurities of OMMPF, especially by reducing the calcium oxalate content.

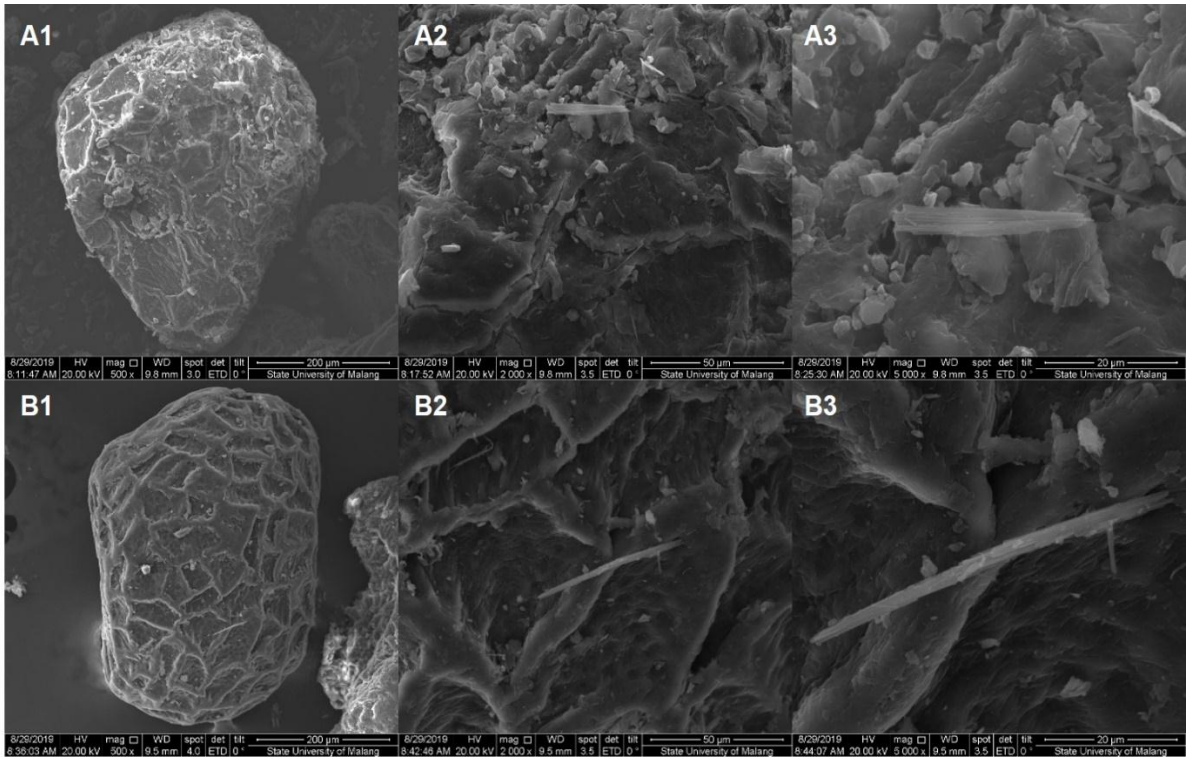

Figure 4 Microstructural analysis of the surface and calcium oxalate crystals of crude (CPF) (A) and optimum micro-mill milled porang flour (OMMPF) (B) with 500x (1), 2000(x) (2), and 5000x (3) magnification

3.2.2 XRD (X-Ray Diffraction)

The XRD analysis is commonly used to determine the level of crystallinity of a food or non-food material. In our study, CPF had an XRD pattern that widened at 2Ø = 10 - 50^0, with the highest peak found at around 21^0, and small peaks at around 16^0 and 38^0, while OMMPF had the highest peak in the surrounding area of 21^0 and small peaks around 37^0 (Figure 5). Similar XRD patterns were found in fresh porang glucomannan (Yanuriati et al., 2017), native sahlep glucomannan (Kurt and Kahyaoglu, 2017b), and native konjac glucomannan (Li et al., 2005). The small peaks at 2Ø = 16^0 in the CPF are related to the presence of starch in the sample (Kurt and Kahyaoglu, 2017a, 2017b), which was not found in the OMMPF samples. It indicates that the dry milling using micro mill assisted separator was also effective in removing starch, which led to a more organized and regular structure of porang flour. Moreover, the increase inthe peak intensity of OMMPF compared to CPF indicates that the dry milling encourages glucomannan molecules to achieve self –crimping and strengthens their interactions (Kurt and Kahyaoglu, 2017b).

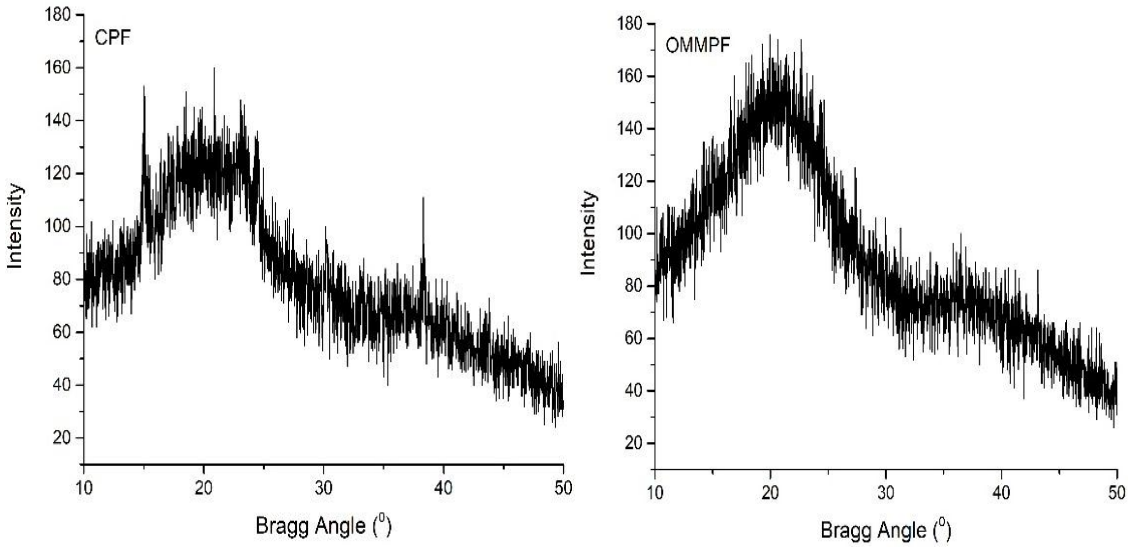

Figure 5 XRD patterns of crude (CPF) and optimum micro-mill milled porang flour (OMMPF)

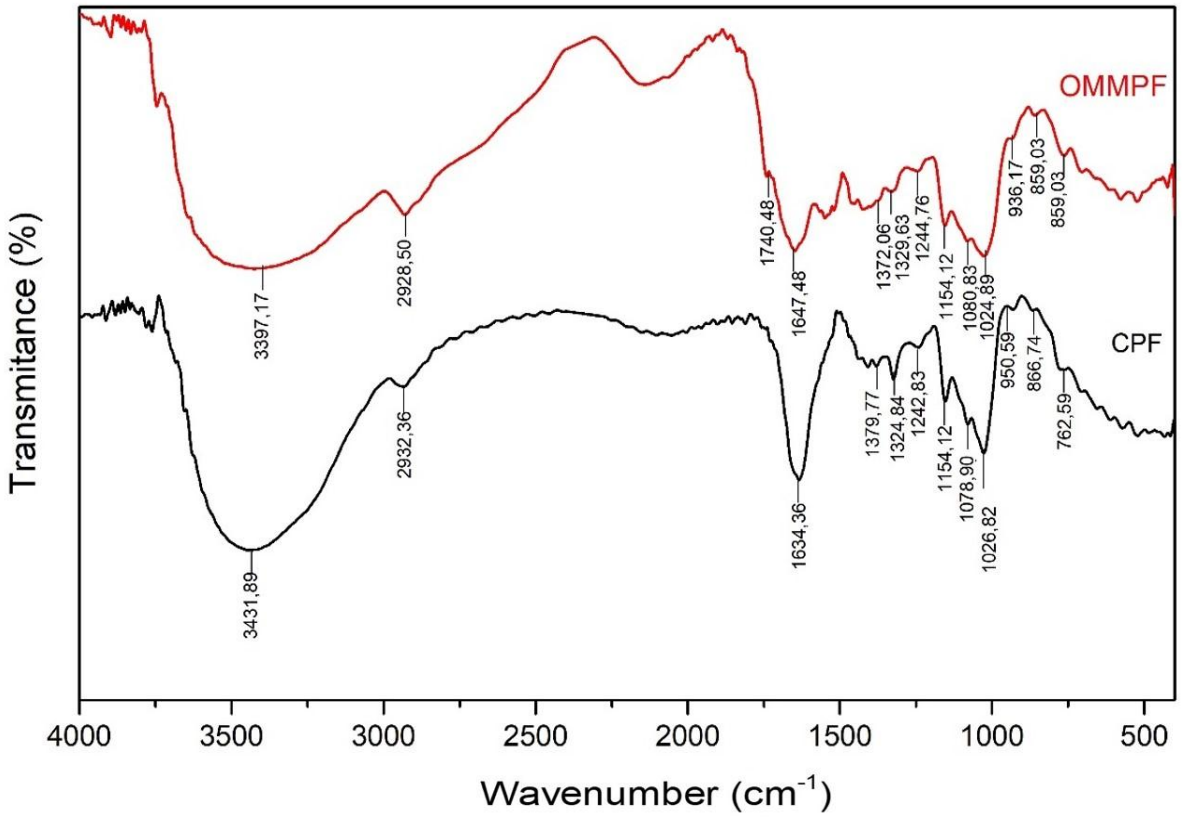

Figure 6 FTIR spectra of crude (CPF) and optimum micro-mill milled porang flour (OMMPF)

3.2.3 FTIR (Fourier-transform Infrared Spectroscopy)

The functional groups of the CPF and OMMPF are shown in Figure 6. The CPF and OMMPF have similar FTIR patterns within the 400 – 4000 cm^{-1} wavenumber range. Broad bands at 3400 cm^{-1} indicate O-H bonds (Zhu et al., 2018) of porang glucomannan. The band at 2900 cm^{-1} has been identified as an asymmetric bond of -CH_2-, while the band at 1634.38 cm^{-1} indicates absorbance of water or protein (Wardhani et al., 2016). Moreover, the bands at 1150 and 1030 cm^{-1} are attributed to C-O-C bonds from the ether group in the pyranose chain, the bands of 1434 cm^{-1} and 1242 cm^{-1} are the bands of C-H,

O-H and CH_2OH, C (=O) O, respectively, whereas the peaks at 1312 cm^{-1}, 1374 cm^{-1}, and 1078 cm^{-1} indicate a C-H bond. The peak at ~1740 cm^{-1} is attributed to C=O stretching vibration (Chua et al., 2012). Furthermore, bands at 800 cm^{-1} and 870 cm^{-1} are attributed to β-mannosidic and β-glucosidic bonds, respectively (Chua et al., 2012; Wardhani et al., 2016). In general, the FTIR patterns of the CPF and OMMPF in this study are in agreement with the results of previous studies by Chua et al. (2012) and Kurt and Kahyaoglu (2017a, 2017b) for konjac glucomannan and sahlep glucomannan as research material, respectively. These results demostrate that the use of feed rate and inlet air velocity as independent variables during the dry milling process of porang chips does not affect the functional groups contained in the porang flour.

3.2.4 Thermal properties

Thermal analysis using DSC identified the CPF and OMMPF as having 2 main peaks. The DSC curves are displayed in Figure 7. The first peak (glass transition peak) were identified at 101.9 ℃ and 99.5 ℃ for CPF and OMMPF, respectively. This result is similar to those from the studies by Li et al. (2005) and Kurt and Kahyaoglu (2017a, 2017b), which stated that the first or endothermic peaks of the native KGM ranged from 50 ℃ - 130 ℃. The first peak indicates the evaporation of water in the porang flour sample. The second peak was observed at 316.8 ℃ in CPF and 310.2 ℃ in OMMPF, which indicates KGM degradation. These results are agreeable with the results of the research conducted by Li et al. (2005) and Wang et al. (2015), who recorded the degradation of KGM occurred at a temperature range of 280 ℃ -340 ℃.

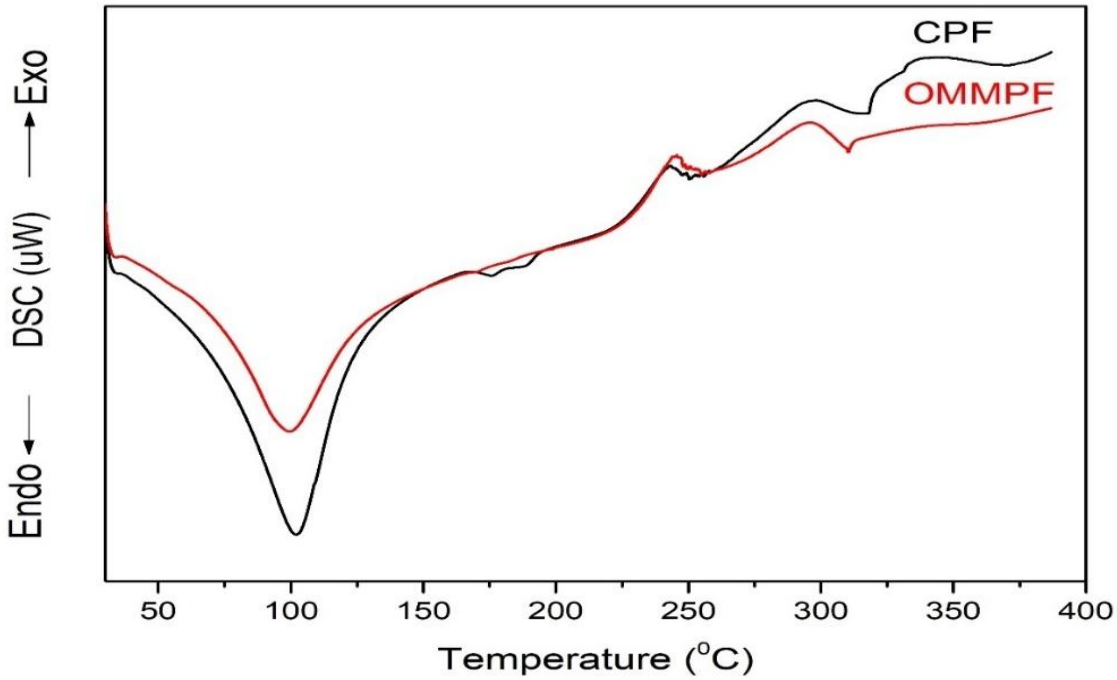

Figure 7 DSC Curves of Crude (CPF) and Optimum micro-mill milled porang flour (OMMPF)

3.2.5 Particle size analysis

The particle sizes of OMMPF are listed in Table 5. The average particle size of OMMPF ranged from 238.63-467.48 μm. The d_{50} of OMMPF was smaller than reported by Li et al. (2005), which stated that the d_{50} of native konjac flour was 657.3 μm.

Table 5 Particle size distribution of optimum micro-mill milled porang flour (OMMPF)

Sample	d_{10} (μm)	d_{50} (μm)	d_{90} (μm)
OMMPF	238.63±1.12	354.66±0.18	467.48±0.12

4 Conclusion

Response surface methodology (RSM) is an excellent tool for optimization of the dry milling of porang chips to produce porang flour. The feed rate and inlet air velocity significantly affected all responses of porang flour examined in this study. The optimum conditions were 48.86 kg h^{-1} of feed rate, and 9 m s^{-1} of inlet air velocity of cyclone separator, for which calcium oxalate response was 2.45%±0.03%, degree of whiteness was 56.90±0.17, viscosity was 4031.30±54.10 cPs, and glucomannan content was 53.29% ±0.22% d.b. However, RSM is suitable for predicting the physicochemical characteristics of porang flour produced by dry milling methods, as reflected by the software prediction and verification values which are not significantly different. Crystallinity degree of porang flour revealed it as having an amorphous pattern. Thermal analysis by DSC showed that porang flour has first and second peaks at 99.5℃ -105.5℃ and 310.2℃ - 316.8℃, respectively. The particle size of OMMPF was in the range of 238.68-467.48 μm, based on evaluation by particle size analyzer. We conclude that the dry milling was effective in reducing impurities and enhanced the glucomannan content, degree of whiteness and viscosity of porang flour. Therefore, the use of micromill-assisted cyclone separator is a viable and promising method for dry milling of porang chips to produce porang flour at a pilot plant and an industrial scale.

Acknowledgement

Parts of this project were funded by the Directorate of Higher Education, Ministry of Research, Technology and Higher Education (RISTEKDIKTI), the Republic of Indonesia through by PMDSU (Pendidikan Magister Menuju Doktor Untuk Sarjana Unggul) Scholarship, underthe contract number: 147/PS2H/LT/DRPM/2018. We also express our deep appreciation and thanks to RISPRO LPDP (Indonesia Endowment Fund for Education), Batch III, for letting us use machinery facilities funded by RISPRO LPDP, without which this research could not have been accomplished.

References

Aderinlewo, A.A., S. A. Ayokambi, L. R. Adetunji, and E. O. Olakunle. 2016. Influence of screen speed and air velocity on the cleaning efficiency of a cowpea rotary screen cleaner. *Journal of Experimental Research*, 4(1): 38–42.

Alonso-Sande, M., D. Teijeiro-Osorio, C. Remuñán-López, and M. J. Alonso. 2009. Glucomannan, a promising polysaccharide for biopharmaceutical purposes. *European Journal of Pharmaceutics and Biopharmaceutics*, 72(2): 453–462.

Al-sadi, J. 2017. Effects of processing parameters on colour variation and pigment dispersion during the compounding in Polycarbonate Grades. In *Annual Technical conference of the Society of Plastics Engineers SPE(ANTEC)*, 515-520. California, Anaheim, USA, 8-10 May.

Avci, A., I. Karagoz, and A. Surmen. 2013. Development of a new method for evaluating vortex length in reversed flow cyclone separators. *Powder Technology*, 235: 460–466.

Baş, D., and I. H. Boyacı. 2007. Modeling and optimization I: Usability of response surface methodology. *Journal of Food Engineering*, 78(3): 836–845.

Basiouny, M. A., and A. E. El-Yamani. 2016. Performance evaluation of two different hammer mills for grinding corn cobs. *Journal of Soil Sciences and Agricultural Engineering*, 7(1): 77–87.

Behera, S. S., and R. C. Ray. 2017. Nutritional and potential health benefits of konjac glucomannan, a promising polysaccharide of elephant foot yam, *Amorphophallus konjac* K. Koch: A review. *Food Reviews International*, 33(1): 22–43.

Central Bureau of Statistics of Madiun Regency. 2018. *Madiun Regency in Figures 2018*. Madiun: Central Bureau of Statistics of Madiun Regency (in Indonesia).

Chen, Y., and Y. Xue. 2019. Optimization of microwave assisted extraction, chemical characterization and antitumor activities of polysaccharides from *porphyra haitanensis*. *Carbohydrate Polymers*, 206: 179–186.

Chiţoiu, M., G.Voicu, G. Paraschiv, G. Moiceanu, V. Vlăduţ, M. Matache, E. Marin, G. Bunduchi, I. Danciu, I. Voicea, and I. Găgeanu. 2016. Energy consumption of a hammer mill when chopping miscanthus stalks. In *Proc. of the 44th International Symposium on Agricultural Engineering: Actual Tasks on Agricultural Engineering*, 215–223. Opatija, Croatia, 23-26 February.

Chua, M., K. Chan, T. J. Hocking, P. A. Williams, C. J. Perry, and T. C. Baldwin. 2012. Methodologies for the extraction and analysis of konjac glucomannan from corms of *Amorphophallus konjac* K. Koch. *Carbohydrate Polymers*, 87(3): 2202–2210.

Faridah, A. 2016. Comperation of porang flour (*Amorphophallus muelleri*) purification method : Conventional maceration (gradient ethanol leaching) and ultrasonic maceration method using response surface methodology. *International Journal on Advanced Science, Engineering Information Technology*, 6(2): 265–272.

Faridah, A., and S. B. Widjanarko. 2013. Optimization of multilevel ethanol leaching process of porang flour (*Amorphophallus muelleri*) using response surface methodology. *International Journal on Advanced Science Engineering Information Technology*, 3(2): 74–80.

Gupta, S. 2013. Process optimization for milling of moong beans *(Vigna radiata)*. M.S. thesis, Punjab: Punjab Agricultural University.

Hermanto, M. B., S. B. Widjanarko, W. Suprapto, and A. Suryanto. 2019. The design and performance of continuous porang (*Amorphophallus muelleri* Blume) flour mills. *International Journal on Advanced Science Engineering Information Technology*, 9(6): 2021–2027.

Impaprasert, R., C. Borompichaichartkul, and G. Srzednicki. 2014. A new drying approach to enhance quality of konjac glucomannan extracted from *Amorphophallus muelleri*. *Drying Technology*, 32(7): 851–860.

Iwuoha, C. I., and F. A. Kalu. 1995. Calcium oxalate and physico-chemical properties of cocoyam (*Colocasia esculenta* and *Xanthosoma sagittifolium*) tuber flours as affected by processing. *Food Chemistry*, 54(1): 61–66.

Kurt, A., and T. Kahyaoglu. 2017a. The physicochemical and structural characteristics of cultivated sahlep. *International Journal of Secondary Metabolite*, 4(3): 488–498.

Kurt, A., and T. Kahyaoglu. 2017b. Purification of glucomannan from salep: Part 2. Structural characterization. *Carbohydrate Polymers*, 169: 406–416.

Li, B., J. Xia, Y. Wang, and B. Xie. 2005. Structure characterization and its antiobesity of ball-milled konjac flour. *European Food Research and Technology*, 221(6): 814–820.

Liu, P. Y., S. L. Zhang, G. H. Zhu, Y. Chen, H. X.Ouyang, and M. Han. 2002. *Professional standard for the classification, requirements and test methods of konjac flour; Technical Report NY/T 494.* Sichuan, P.R. China.

Manab, A., H. Purnomo, S. B. Widjanarko, L. E. Radiati, and I. Thohari. 2017. Physichochemical properties of kefir drink using modified porang flour (*Amorphophallus oncophyllus*) during storage period. *Current Research in Nutrition and Food Science*, 5(3): 288–299.

Marinuc, M., and F. Rus. 2011. Effect of particle size and input velocity on cyclone separation process. *Bulletin of the Transilvania University of Brasov Series II: Forestry, Wood Industry, Agricultural Food Engineering*, 4(53): 117–122.

Mawarni, R. T., and S. B.Widjanarko. 2015. Grinding by ball mill with chemical purification on reducing oxalate in porang flour (In Indonesia). *Food and Agroindustrial Journal*, 3(2): 571–581 (in Indonesia).

Pasandide, B., F. Khodaiyan, Z. E. Mousavi, and S. S. Hosseini. 2017. Optimization of aqueous pectin extraction from *Citrus medica* peel peels. *Carbohydrate Polymers*, 178: 27–33.

Scanlon, M. G., and J. E. Dexter. 1986. Effect of smooth roll grinding conditions on reduction of hard red spring wheat farina. *Cereal Chemistry*, 63(5): 431–435.

Simonyan, K. J., Y. D.Yiljep, and O. J. Mudiare. 2006. Modeling the grain cleaning process of a stationary sorghum thresher. *CIGR Journal*, 8: PM06012.

Sugiono, S., M. Masruri, T. Estiasih, and S. B. Widjanarko. 2019. Optimization of extrusion-assisted extraction parameters and characterization of alginate from brown algae (*Sargassum cristaefolium*). *Journal of Food Science and Technology*, 56(8): 3687–3696.

Surjosatyo, A., A. Respati, H. Dafiqurrohman, and Muammar. 2017. Analysis of the influence of vortexbinder dimension on cyclone separator performance in biomass gasification system. *Procedia Engineering*, 170: 154–161.

Tatirat, O., and S. Charoenrein. 2011. Physicochemical properties of konjac glucomannan extracted from konjac flour by a simple centrifugation process. *LWT - Food Science and Technology*, 44(10): 2059–2063.

Tumuluru, J. S., L. G. Tabil, Y. Song, K. L. Iroba, and V. Meda. 2014. Grinding energy and physical properties of chopped and hammer-milled barley, wheat, oat, and canola straws. *Biomass and Bioenergy*, 60: 58–67.

Ukpabi, U.J., and J.I. Ejidoh. 1989. Effect of deep oil frying on the oxalate content and the degree of Itching of cocoyams (*Xanthosoma* and *Colocasia* spp). In *5th Annual Conference of The Agricultural Society of Nigeria*. Federal University of Technology, Owerri, Nigeria, 3-6 Sept.

Uzombah, T. A., and S. O. Awonorin. 2010. Effects of particle size and moisture content on the apparent viscosity of pastes of

some reconstituted indigenous flours. *Nigerian Food Journal*, 28(2).

Wang, C., M. Xu, W. Lv, P. Qiu, Y. Gong, and D. Li. 2012. Study on rheological behavior of konjac glucomannan. *Physics Procedia*, 33: 25–30.

Wang, L. 2004. Theoretical study of cyclone design. Ph.D. Diss., Texas: Texas A&M University.

Wang, S., B. Zhou, Y. Wang, and B. Li. 2015. Preparation and characterization of konjac glucomannan microcrystals through acid hydrolysis. *Food Research International*, 67: 111–116.

Wardhani, D. H., F. Nugroho, M. Muslihudin, and N. Aryanti. 2016. Application of response surface method on purification of glucomannan from *Amorphophallus oncophyllus* by using 2-propanol. *Scientific Study and Research: Chemistry and Chemical Engineering, Biotechnology, Food Industry*, 17(1): 63–74.

Widjanarko, S. B., A. Faridah, and A. Sutrisno. 2014. Optimization of ultrasound-assisted extraction of konjac flour from *Amorphophallus muelleri* blume. In *Gum and Stabilisers for the Food Industry 17: The Changing Face of Food Manufacture: The Role of Hydrocolloids* eds P. A. Williams, and G. O. Phillips, ch. 2, 109–121. Wales, United Kingdom: The Royal Society of Chemistry.

Widjanarko, S. B., A. Nugroho, and T. Estiasih. 2011. Functional interaction components of protein isolates and glucomannan in food bars by FTIR and SEM studies. *African Journal of Food Sciences*, 5(1): 12–21.

Widyaningsih, T. D., S. B.Widjanarko, E. Waziiroh, N. Wijayanti, and Y. L. Maslukhah. 2018. Pilot plant scale extraction of black cincau (*Mesona palustris* BL) using historical-data response surface methodology. *International Food Research Journal*, 25(2): 712–719.

Witoyo, J. E., S. B. Widjanarko, and B. D. Argo. 2019. The effect of feed rate and inlet air velocity to reduce calcium oxalate on porang chips using micro mill assisted Cyclone separator. *AIP Conference Proceedings*, 2120(1): 050013.

Xu, W., S. Wang, T. Ye, W. Jin, J. Liu, J. Lei, B. Li, and C.Wang. 2014. A simple and feasible approach to purify konjac glucomannan from konjac flour - Temperature effect. *Food Chemistry*, 158: 171–176.

Yanuriati, A., D. W Marseno, Rochmadi, and E. Harmayani. 2017. Characteristics of glucomannan isolated from fresh tuber of Porang (*Amorphophallus muelleri* Blume). *Carbohydrate Polymers*, 156: 56–63.

Zhang, C., J. Chen, and F. Yang. 2014. Konjac glucomannan, a promising polysaccharide for OCDDS. *Carbohydrate Polymers*, 104: 175–181.

Zhu, C., and X. Liu. 2013. Optimization of extraction process of crude polysaccharides from Pomegranate peel by response surface methodology. *Carbohydrate Polymers*, 92(2): 1197–1202.

Zhu, W., J. Li, J. Lei, Y. Li, T. Chen, T. Duan, W. Yao, J. Zhou, Y. Yu, and Y. Liu. 2018. Silver nanoparticles incorporated konjac glucomannan-montmorillonite nacre-like composite films for antibacterial applications. *Carbohydrate Polymers*, 197: 253–259.